2021

Experimental Evaluation of Local Air-side Heat Transfer Coefficient on Single Fins

Min Che
University of Illinois Urbana-Champaign, minche2@illinois.edu

Stefan Elbel

Experimental Evaluation of Local Air-Side Heat Transfer Coefficient on Single Fins

Min CHE[(a)], Stefan ELBEL[(a,b,*)]
[(a)] Air Conditioning and Refrigeration Center,
Department of Mechanical Science and Engineering,
University of Illinois at Urbana-Champaign,
1206 West Green Street, Urbana, IL 61801, USA
[(b)] Creative Thermal Solutions, Inc.,
2209 North Willow Road, Urbana, IL 61802, USA
[(*)] Corresponding Author
Email: elbel@illinois.edu

ABSTRACT

Quantification of local air-side heat transfer coefficient (HTC) on fin-and-tube heat exchanger fins is a challenging task, especially when the fin geometry is complex. A newly developed experimental method can obtain two-dimensional HTC distribution on fin surfaces with a high resolution (8.9 μm). In this research, a thin (20 μm) yellow coating is sprayed on the surface of the fins. The coated fins were exposed in the wind tunnel which has the tracer gas (50 ppm_v ammonia) well mixed in the airflow. During the experiment, the color of coated surface changes from yellow to blue. The rate of local mass transfer is correlated with the rate of local color change. Then, by applying the analogy between heat and mass transfer, local HTCs on the fin surfaces are quantified. The method accuracy has been validated on fundamental shapes such as flat plates, and cylinders. Two-dimensional HTC distributions on a four-row wavy fin and a four-row slit fin have been obtained by employing this new method. As there is no local measurement on these geometries exists, the averaged HTCs on the fin surfaces have been critically compared to the averaged HTCs from entire heat exchanger measurements from the literature. This method has provided an accurate, robust, and inexpensive tool to evaluate local air-side HTCs for real-scale heat exchangers with complex fin geometry and multiple tube rows.

1. INTRODUCTION

Fin-and-tube heat exchanger is the most common design in the HVAC&R industry due to its compactness in structure and low cost. According to Joardar and Jacobi (2005), air-side convective resistance is the most significant contributor to the total heat transfer resistance in refrigerant-to-air heat exchangers. Plain fin is the basic fin geometry that extends the surface area to increase the air-side heat transfer. Although it has a relatively low heat transfer performance in comparison to more enhanced designs, the advantages of low pressure drop, and high reliability are still valued in many application areas today. Therefore, it is still being employed in the air-conditioning and refrigeration industry. Wavy fins enhance the mixing of the airflow in the channel in order to improve the convective heat transfer. Wang *et al*. (1997) have evaluated different types of wavy fins and compared them with the plain fin. They have concluded that the averaged HTC of the wavy fin is more than 50% higher than its plain fin counterpart. The surface geometry of the louver fin and slit fin interrupts the main flow and is designed to periodically restart the boundary layer. This mechanism by far is the most effective method to enhance air-side heat transfer. However, the pressure drop penalty is high, which increases the power consumption of the blower or fan.

Experimental and computational s are two main methods to evaluate air-side HTCs of fin-and-tube heat exchangers. The Wilson Plot Method was proposed by Wilson (1915) a century ago and is still widely used today to obtain the averaged HTCs. The entire heat exchanger needs to be made and installed in the environmental wind tunnel, effectiveness-NTU (Ɛ-NTU) method is often employed to estimate air-side HTCs by measuring the fluid in the tube side. However, it is only possible to obtain an averaged HTC. Che and Elbel (2019) have reviewed and summarized the main experimental methods to quantify local HTCs. According to Che and Elbel (2019), scaled-up fin samples

are normally used, sample preparation and experimental procedure are usually complex. Moreover, the resolution and accuracy of measurement are often unsatisfied. They have shown the difficulties of applying these methods to obtain local HTCs for real-scale fins with complex geometry and entire heat exchangers. Therefore, CFD simulation is often used in the past decade to evaluate new fin designs and to obtain HTC distribution on fin surfaces. Due to the complexity of the numerical model and the long calculation time, a single fin unit is usually modeled. The entire heat exchanger has been considered as symmetric and periodically duplicate of the single unit. As a result, the model does not represent the actual flow condition of a real heat exchanger. The averaged HTCs on the single fin surfaces from CFD models are used to compare with the experimental results of entire heat exchangers. With the neglection of interaction between adjacent rows and influence from upstream flow, it is not uncommon to see disagreements between CFD and experimental results. For instants, Chu *et al.* (2009) have built a CFD model of a 7-row inline arranged plain fin which is compared to the experimental data of the same geometry from Joardar and Jacobi (2005). The Model overestimated the HTCs at Reynolds number smaller than 600 and underestimated at Reynolds number larger than 700. Chimres *et al.* (2018) have applied the computational method to optimize the design parameters of a semi-dimple VG on a plain fin. Their base model of a unit fin with VG has been compared to the experimental results of the same geometry from Wang *et al.* (2015). The averaged HTCs have been underestimated at Reynolds numbers smaller than 1200 and overestimated at Reynolds numbers larger than 2500. However, there is no convincible explanation for the deviations. Therefore, an experimental method to investigate local HTCs of fins is desired to verify and improve the CFD models.

Che and Elbel (2019) have proposed an experimental method called coating, tracer, and color change (CTC) to visualize and quantify local air-side HTCs for all kinds of surfaces. As shown in Figure 1, the process involves a thin, acidic coating on the substrate surface (aluminum, copper, stainless steel, and plastic have been tried) which is exposed to a low concentration of ammonia tracer gas mixed with flowing air. The coating absorbs ammonia and water vapor and gradually changes color from yellow to blue. By quantifying the change of color, the local mass transfer can be obtained. Local HTCs can be subsequently calculated.

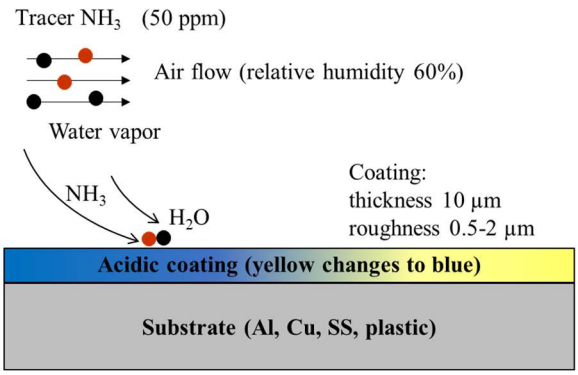

Figure 1: Principle of the CTC method - Che and Elbel (2019)

The current study has upgraded the coating material and utilized a spray coating method. The purpose is to improve coating uniformity and to reduce experimental uncertainty. Moreover, the spray coating method can be used for fins with complex surface geometry such as a real-scale louver fin. The method accuracy has been verified on fundamental geometries in the current study. The measured local HTCs show good agreement compared to the analytical solutions and measurements found in the literature. Furthermore, the method has been evaluated under a wide range of conditions by Che and Elbel (2019) including flow velocities ranging from 0 to 5 ms^{-1}, airflow temperatures from 15 to 55°C, relative humidity from 60% to 95%, and volumetric ammonia concentrations from 15 to 85 ppm_v. Therefore, the improved CTC method has been proved to be a robust tool to evaluate the air-side HTCs for all kinds of real-scale heat exchanger fins. In the current study, two-dimensional HTC distributions of a four-row wavy fin and a four-row slit fin have been obtained experimentally by utilizing the CTC method. By taking mathematical mean on the entire fin surface, averaged HTC of the surface can be obtained. The results have been critically compared to the averaged HTCs from measurements in the literature of similar geometry. This new method can fill the gap between the current CFD model and experimental results on evaluating heat exchanger performance; interpret the local heat transfer enhancement due to surface geometries, generate more accurate correlations for heat exchangers, and find new opportunities to enhance air-side heat transfer.

2. METHODOLOGY

2.1 Analogy between Heat and Mass Transfer

According to Bejan (1995), the analogy between heat and mass transfer has been well-accepted in many kinds of flow such as laminar flow, turbulent flow through flat and no-flat surfaces, duct flow, and natural convection. Schematics of boundary layers of laminar flow over a flat plate are shown in Figure 2. The assumptions include incompressible fluid, no-slip, and an impermeable wall which are well accepted for laminar flow over a solid plate. Figure 2 (a) shows the convection heat transfer boundary layer with a constant temperature difference while Figure 2 (b) shows the convection mass transfer boundary layer with a constant concentration difference. For the low concentration (50 ppm_v ammonia) mass transfer, the impermeable-surface assumption is still valid.

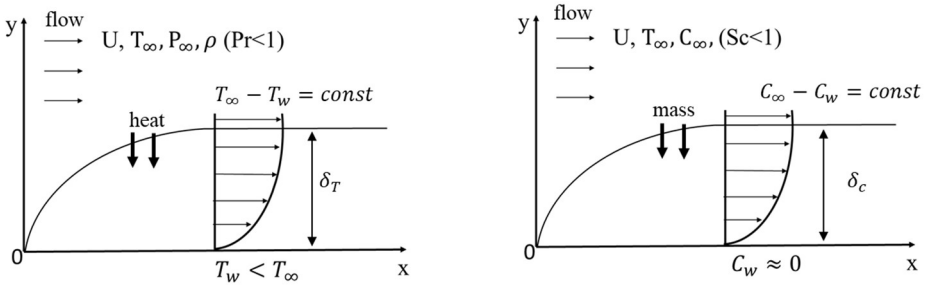

Figure 2: Convection heat and mass transfer analogy in the boundary layer of laminar flow over a flat plate, (a) Heat transfer boundary layer with constant ΔT, (b) Mass transfer boundary layer with constant ΔC

Local HTC (h_{loc}) can be quantified by measuring local heat flux at a constant temperature difference shown in Equations (1). The mass transfer has a similar manner that local mass transfer coefficient (h_{mloc}) can be determined by quantifying local mass flux at a known concentration difference shown in Equations (2). As shown in Equation (3), dimensionless heat transfer Nusselt number (Nu) is a function of Reynolds number (Re) and Prandtl number (Pr), while dimensionless mass transfer Sherwood number (Sh) is a function of Reynolds number (Re) and Schmidt number (Sc). For air at 26°C, 60% relative humidity (RH), 101 kPa, and dilute ammonia-in-air, the analogy relation between heat transfer and mass transfer is approximately equal to 1 (n=1/3 for laminar flow, n=0.4 for turbulent flow) as shown in Equation (4).

$$h_{loc} = \frac{\dot{q}_{loc}}{\Delta T_{loc}} \; ; \quad Nu_{loc} = \frac{h_{loc} x}{k_f} \tag{1}$$

$$h_{mloc} = \frac{\dot{m}_{loc}}{\Delta C_{loc}} ; \; Sh_{loc} = \frac{h_{mloc} x}{D} \tag{2}$$

$$Nu = BRe^m Pr^n ; \; Sh = BRe^m Sc^n \tag{3}$$

$$\frac{Sh_{loc}}{Nu_{loc}} = \left(\frac{Sc}{Pr}\right)^n = \left(\frac{0.75}{0.74}\right)^n \approx 1.00 \tag{4}$$

2.2 Procedure to Obtain Local HTCs

Che and Elbel (2019) have developed an image processing algorithm using MATLAB R2018a to quantify the local color change. By using the procedure outlined in Figure 3, two-dimensional HTC distributions can be obtained for the surface of interest. Hue value is used to quantify the color of the coating before (yellow) and after (blue) the chemical reaction takes place. In Equation (5), the local HTC is proportional to the rate of color change (ϵ/t). Here M_{max}/A_{tot} is the ammonia absorption capability per unit surface area which can be determined from the mass of the coating material, the surface area, and chemical relation between the coating material and the ammonia gas; S is the color change factor (S) which is obtained by calibration; k_f is the thermal conductivity of air; D is the diffusion coefficient of dilute ammonia-in-air; ΔC is the concentration difference between the free stream and the wall. Therefore, in Equation (5) all parameters in the parentheses are constant.

$$h_{loc} = \left(\frac{S \cdot M_{max} \cdot k_f}{A_{tot} \cdot \Delta C \cdot D}\right) \cdot \frac{\epsilon}{t} \tag{5}$$

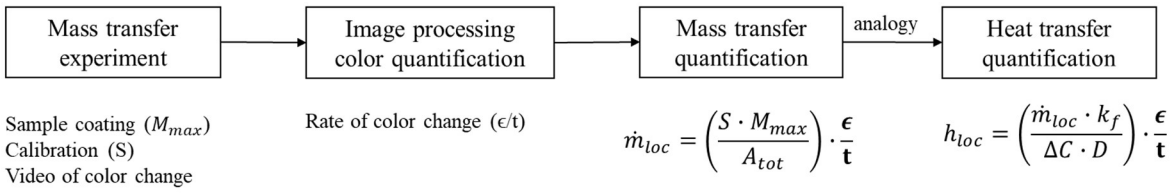

Figure 3: Procedure to obtain two-dimensional HTC distribution

3. EXPERIMENTAL SETUP AND PROCEDURE

3.1 Experimental Setup

A suction-type open-loop wind tunnel that meets the requirements of ASHRAE Standard 41.2-1987 (RA 92) has been employed for the mass transfer experiments and shown in Figure 4. The size of the test section is W120 mm x H100 mm x L400 mm. The flow velocity across the test section can be adjusted from 0 to 5 ms^{-1}. The airflow, water vapor, and anhydrous ammonia are injected at the entrance. A CCD camera is employed for image recording. An electrochemical gas sensor is connected to the test section to obtain real-time volumetric ammonia concentration. Standard ASME nozzles are used to measure flow rate and velocity across the test section. Downstream of the nozzle, a relative humidity sensor is employed to track and control the humidity of the flow. Differential pressure transducers are used to measure pressure drop at the test section and the nozzle.

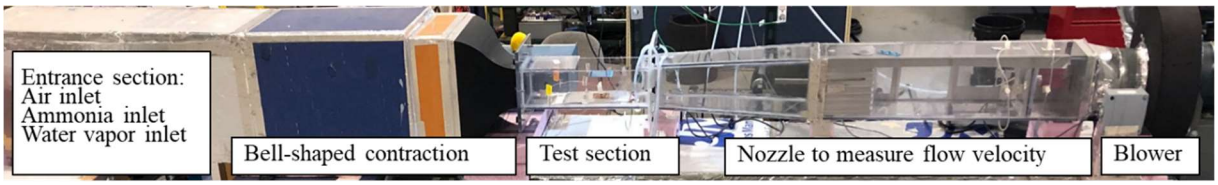

Figure 4: Open-loop wind tunnel for conducting mass transfer experiment

Table 1 shows the parameters of measurements and their uncertainties. Type B uncertainty is evaluated accordingly by using Equations (5) and (6) and is 12%.

$$Y_{h_{loc}} = \left\{\sum_i \left(\frac{\partial h_{loc}}{\partial X_i} \cdot Y_i\right)^2\right\}^{1/2} \tag{6}$$

Table 1: Uncertainty of measurements

Parameter	Sensor	Units	Range of test	Uncertainty
Airflow temperature	Type-T thermocouples	°C	-7 to 55	± 0.3
Relative humidity	Humidity transmitter	%	0 to 100	± 5% reading
Pressure drop	Differential pressure transducer	Pa	± 62	± 1% FS
Pressure drop	Differential pressure transducer	Pa	± 622	± 1% FS
Airflow velocity	Flow nozzle	Ms^{-1}	0 to 5	± 1% reading
Ammonia concentration	Electrochemical	ppm_v	0 to 100	± 10% reading

3.2 Experimental Procedure

Figure 5 (a) shows the fin array sample at the test section. A CCD camera is located above the sample at a distance of 2.5 m from the coated surface to have a high-quality top view image of the entire fin surface. Two 25 W white LED lights are used to maintain a consistent illumination. First, the coating material is sprayed onto a single fin surface. The coated fin initially shows a bright yellow color and is then installed into the fin array as shown in Figure 5 (b). Copper tubes are installed, and the surfaces of the tubes are wrapped with tape to make sure the contact between the tubes and fins is tight. In addition, two rods are used to align the top assembly with the bottom assembly. The cross-sectional area of the fin array is the same as the cross-sectional area of the test section. Therefore, the fin array assembly can represent the same flow condition as an entire heat exchanger. It is important to locate the coated fin in

the middle of the array to have a uniform flow velocity and tracer concentration for the steady-state mass transfer experiment. The fin array sample can be used to measure both heat transfer and pressure drop in the experimental setup. It is worth mentioning that the mass transfer and color change will not happen if no tracer gas (ammonia) is injected into the airflow. Therefore, the sample is waiting in the test section until a stable condition is obtained (flow temperature, relative humidity, and velocity). Afterward, the ammonia valve is opened for a pre-set time step such as 30 seconds. Images of the surface after each time step are recorded by the camera by removing the top layer of the fin array. This procedure has been repeated until the entire coated surface changes to a blue color. Therefore, the images of color change (ϵ) at a different time (t) are obtained for calculating local HTCs.

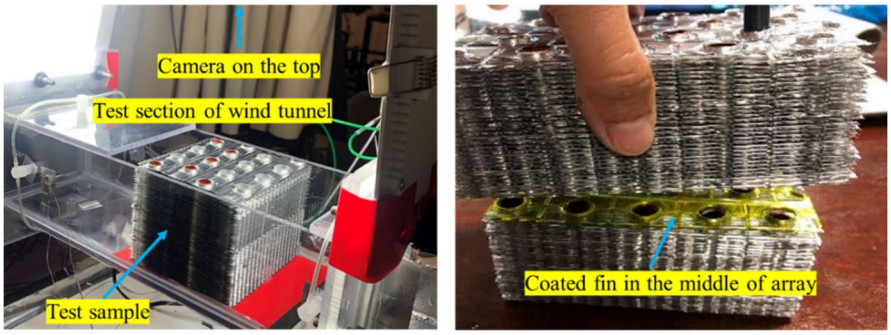

(a) Sample at test section (b) Coated fin in the middle of array

Figure 5: Sample preparation, (a) Fin array at test section, (b) Coated fin in the middle of the array

4. METHOD VALIDATION ON FUNDAMENTAL GEOMETRIES

4.1 Laminar Flow over a Flat Plate

As laminar flow over a flat plate has a well-accepted analytical solution (Blasius solution), the accuracy of the CTC method has been evaluated by comparing it with the Blasius solution as shown in Figure 6. The flat plate sample is L50 x W50 x T0.5 mm in size and made of aluminum with AMS 71 coating material (manufactured by Serionix, Inc.). The coating thickness and uniformity have been measured by employing a Laser Scanning Confocal Microscope (Keyence VK-X1000) which is 20 ±2 µm. The experimental condition is airflow at 26 ºC, 60% RH at 1 ms^{-1} velocity, ammonia concentration is 50 ppm_v. Figure 6 shows both two-dimensional HTC distribution of one sample and span-averaged HTCs of multiple measurements. The results show good accuracy and repeatability compared to the Blasius solution except for the leading and trailing edges. Blasius solution is based on the boundary layer equation which assumes the length of the plate is much larger than the thickness of the boundary layer. Therefore, it does not hold at the leading edge. At the trailing edge, the boundary layer is discontinuous, the streamwise velocity gradient is not negligible. Therefore, the measured HTCs at the edges represent the real situation.

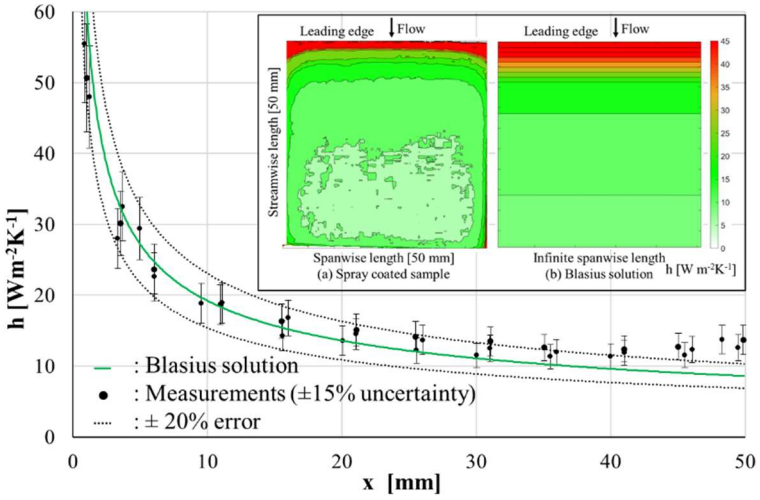

Figure 6: Local HTCs comparison between measurements and Blasius solution (Re_L=3109)

4.2 External Flow across Cylinders

Fluid passing a cylindrical surface is observed in all kinds of engineering applications such as heat exchangers, turbines, and airfoils. Therefore, heat transfer of external flow across cylinders has been investigated since the early 1900s. In the current study, cylinders of different outer diameters have been investigated. The length of the cylinders is the same as the width of the test section and has been fixed in the wind tunnel at both ends. At each of the two ends, the cylinder is covered with paper tape. Angles (θ) from 0 to 360º along the cylinder surface are marked on the tape as shown in Figure 7. Due to cylinder symmetry, only half of the cylinder (0 to 180°) has been analyzed to obtain local HTCs. As shown in Figure 7 (b), the color change starts from the stagnation region in front of the cylinder and spreads along the surface in the circumferential direction. Flow separation has been observed between 80 to 110°, and flow reattachment is seen at the back (120 to 180°) as shown in Figure 7 (c).

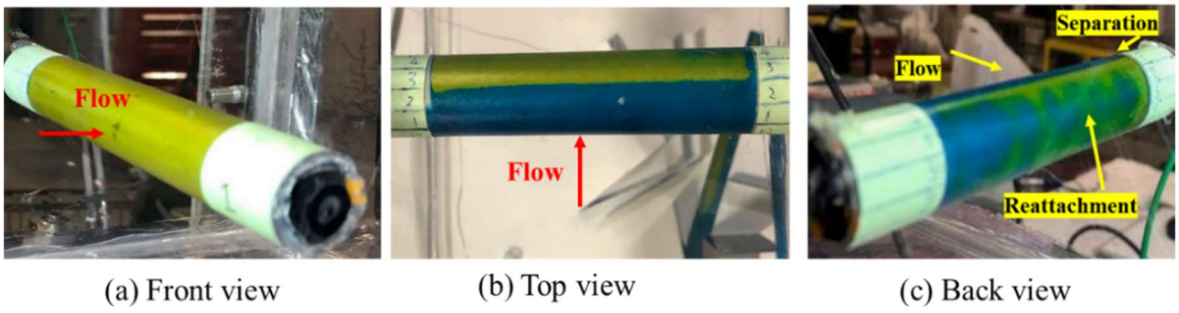

Figure 7: Color change observation of a cylinder, (a) Front view when t=0 s, (b) Top view, (c) Back view

Figure 8 shows the measured span-averaged HTCs at Re_d=4780 and its comparison with results in the literature. The measurements of the current study agree with the measurements from Krall and Eckert (1973) and the analytical solution of Goland (1950) before the separation point. The analytical solution is only available before the flow separation because flow motion is too complex at the wake region at high Re numbers. In the aspect of the experiment, the experimental condition of Krall and Eckert is based on uniform heat flux, while the current study is based on a uniform surface temperature. Moreover, Krall and Eckert have used thermocouples to measure temperature distribution at a single position on the cylinder, while span-averaged HTCs are used in the current study.

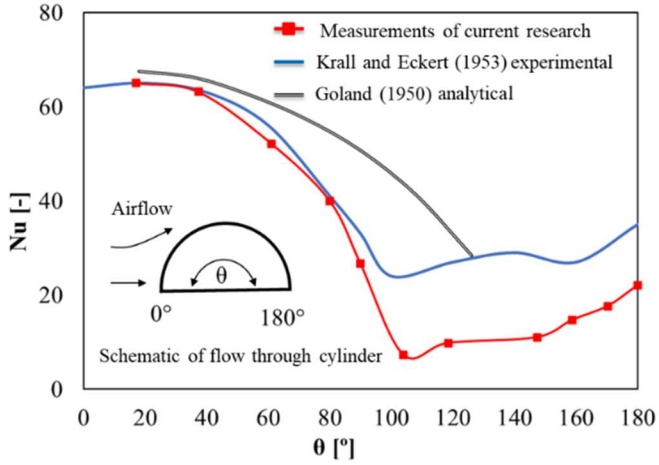

Figure 8: Measurements of local Nu numbers along the cylinder surface at Re_d=4780

5. EXPERIMENTAL RESULTS OF FIN ARRAYS

5.1 Two-Dimensional HTC Distribution of a Sine Wave Fin and a Slit Fin

Two real-scale fins with 20 μm coating are shown in Figure 9. They have identical tube diameter (D_o=12.7 mm), transverse (P_t=31.75 mm) and longitudinal (P_l=27.5 mm) tube distance, staggered tube arrangement, and four tube rows. For the sine wave fin shown in Figure 9 (a), the wave height P_d is 2 mm. For the slit fin shown in Figure 9 (b), there are 10 slots for each tube row, and the maximum slit height L_d is 1.4 mm.

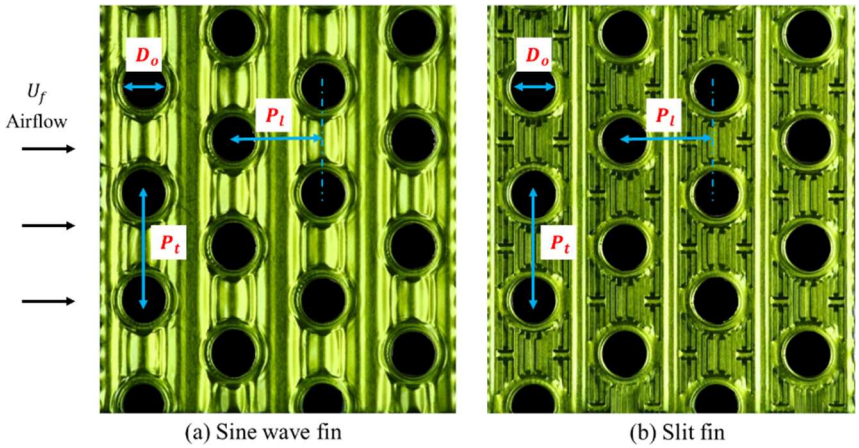

Figure 9: Fin shape and geometric parameter for local HTC investigation, (a) Sine wave fin, (b) Slit fin

Color change images of the sine wave fin and the slit fin with staggered tube arrangement are shown in Figure 10 under the same experimental condition. The time step of image recording is 30 s. Longer or shorter time steps can be selected for lower or higher flow velocities and ammonia concentrations. In Figure 10, a faster color change represents a higher HTC. The first row changes color faster due to the leading-edge effect for both fin types. For the sine wave fin, the hills of the wave show a faster color change compared to the valleys. Flow separation at the backside of the tubes is observed. For the slit fin, the slits restart the boundary layer to maximize the leading-edge effect. This agrees with the observation in Figure 10 that the overall color change of the slit fin is faster than the sine wave fin.

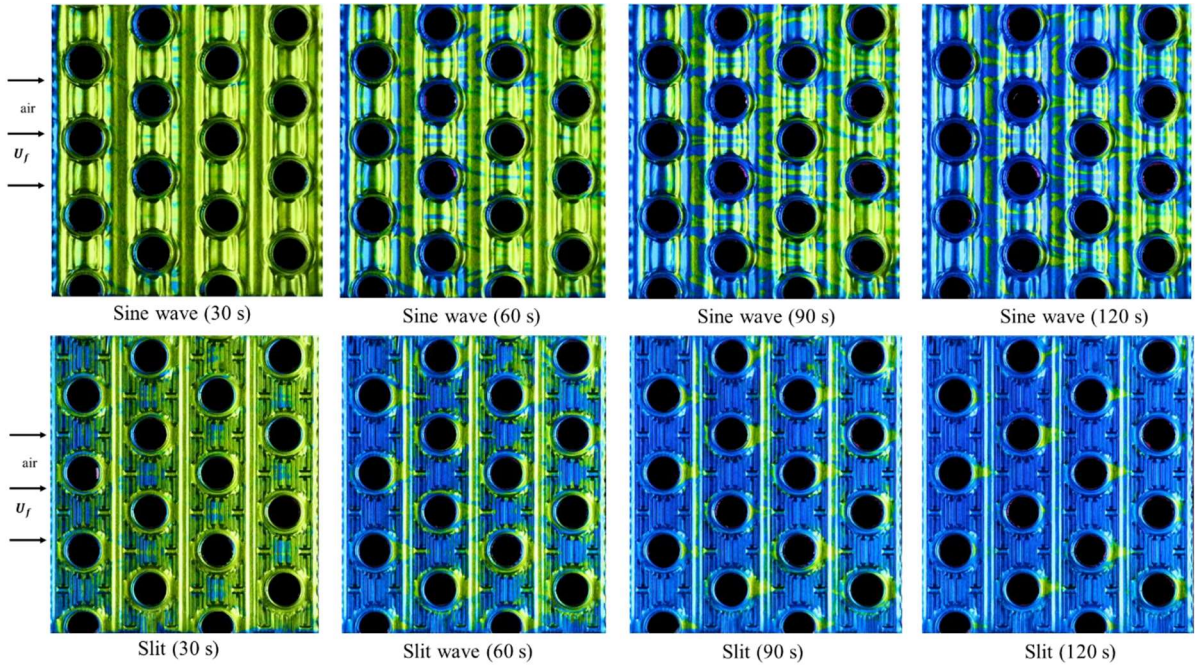

Figure 10: Color change images of the sine wave and slit fin (U_f=2 ms^{-1}, Re_{Dc}=2815)

The two-dimensional HTC distributions of the two fins at the same experimental condition are shown in Figure 11. The quantified HTCs agree with the color change observation shown in Figure 10. Local HTCs of each pixel on the fin surfaces have been obtained. Therefore, averaged HTCs can be calculated via simple math. The averaged HTC of the slit fin is 64% higher than the sine wave fin at the same flow velocity. However, the pressure drop penalty is high. In Fig. 11, there are 1181 x 1308 pixels on the 110 x 125 mm surface. Therefore, the resolution of the color change observation is 8.9 μm, which represents the resolution of the local HTC evaluation. Local HTC distributions of the two fin samples are also investigated under different face airflow velocities.

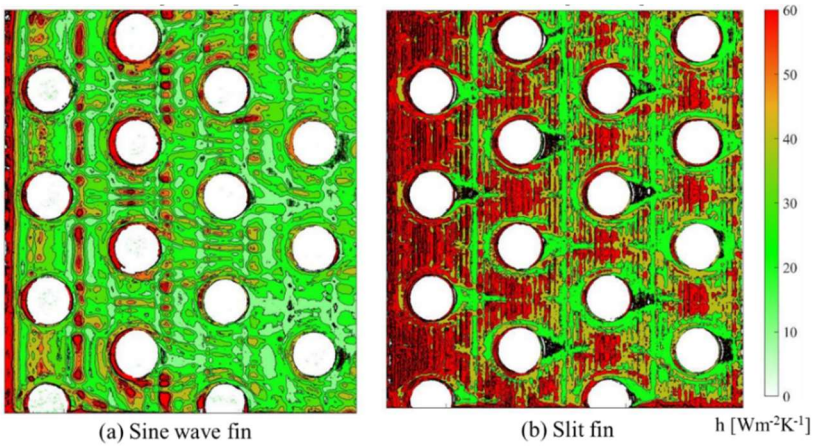

Figure 11: Tow-dimensional HTC distributions (U_f=2 ms^{-1}, Re_{Dc}=2815)

5.2 Averaged HTCs and pressure drop comparison with results in the literature

The air-side performance of heat exchangers is often described by heat transfer Colburn *j* factor and friction factor *f* because the enhancement of heat transfer typically comes at the expense of increased pressure drop. Therefore, pressure drops have been measured in the current study as well. Fin collar outside diameter (D_c) is used as the characteristic length. The data reduction for *j* and *f* factors is shown in Equations (7) to (9) according to Wang *et al*. (2000) and Kays and London (1984). U_{max} is the maximum air velocity in the tube bank.

$$Re_{Dc} = \frac{U_{max} D_c}{\nu} \tag{7}$$

$$j = \frac{\overline{Nu}}{Re_{Dc} \cdot Pr^{1/3}} \tag{8}$$

$$f = \frac{A_c}{A_{tot}} \cdot \frac{\rho_m}{\rho_1} \left[\frac{2\rho_1 \cdot \Delta P}{\dot{m}^2} - (1+\sigma^2)\left(\frac{\rho_1}{\rho_2} - 1\right) \right]; \; \dot{m} = U_{max} \cdot \rho_m \tag{9}$$

There is no local HTC measurement of fin arrays like the current study. Therefore, averaged heat transfer and pressure drop of the current study have been compared with measurements in literature and shown in Figure 12. The heat exchangers evaluated by Wang *et al*. (1999) and Jabardo *et al*. (2006) have similar geometric parameters as the current study. They have the same tube diameter, transverse and longitudinal tube distances, staggered tube arrangement, and four tube rows. In Figure 12 (a), the wavy fin used in the current study has a sine wave shape, while both Wang and Jabardo's group have measured the fins of the triangular wave shape. In Figure 12 (b), averaged heat transfer and pressure drop of the slit fin have been compared to the results of louver fins from two research groups. The fin pitch in the current study is the same as the fin used by Okbaz *et al*. (2020).

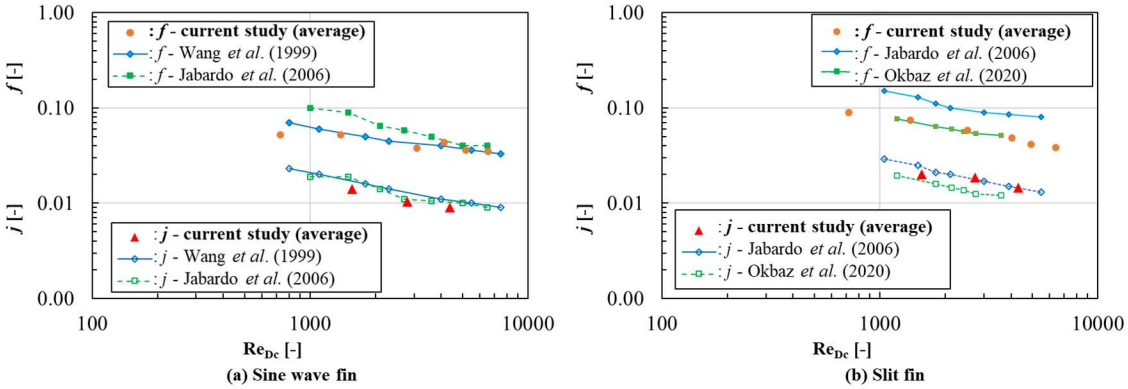

Figure 12: Averaged heat transfer and pressure drop in the current study compared to results in the literature, (a) Sine wave vs. triangular wave, (b) Slit fin vs. louver fin

6. CONCLUSION AND FUTURE WORK

The improved CTC method has been employed to obtain two-dimensional HTC distributions on real-scale heat exchanger fin surfaces. The accuracy of this method has been verified on both fundamental geometries (15% compared to Blasius solution on flat plates) and commonly used heat exchanger fins. The new CTC method has several advantages:

- Applicable for real-scale metal fins of complex geometry.
- High accuracy (within 15% uncertainty), high resolution (8.6 μm) HTC, and robust.
- Easy sample preparation and data reduction, reusable samples, and low-cost experimental setup.

It is promising to be used in the following area with further validation and improvements.

- Generate row-by-row correlations of air-side HTCs for dry surfaces of heat exchangers.
- Verify local HTCs from CFD models and improve the accuracy of CFD models.
- Fin geometry optimization and suggestion better fin designs.

Some improvements need to be addressed such as involving fin efficiency, controlling, and evaluating coating uniformity. The CTC method provides a powerful tool to study air-side heat transfer on complex surfaces.

NOMENCLATURE

Symbols and Abbreviations

A	Surface area (m^2)	$\dot{q}$	Heat flux ($W\ m^{-2}$)
AMS 71	coating material designation (-)	Re	Reynold number (-)
B	Constant (-)	RH	Relative humidity (%)
CFD	Computational fluid dynamics (-)	S	Color change factor (-)
CTC	Coating, tracer, and color change (-)	Sc	Schmidt number (-)
C	Concentration ($kg\ m^{-3}$)	Sh	Sherwood number (-)
D	Diffusion coefficient ($m^2\ s^{-1}$)	T	Temperature (K)
D_o	Tube outer diameter (mm)	t	Time (s)
D_c	Fin collar outside diameter (mm)	U	flow velocity ($m\ s^{-1}$)
f	Friction factor (-)	U_f	Face airflow velocity ($m\ s^{-1}$)
FS	Full scale (-)	x	Streamwise dimension (m)
HTC	Heat transfer coefficient ($W\ m^{-2}\ K^{-1}$)	ρ	Air density ($kg\ m^{-3}$)
h	Heat transfer coefficient ($W\ m^{-2}\ K^{-1}$)	ϵ	Ratio of color change (-)
h_m	Mass transfer coefficient ($kg\ m^{-2}\ s^{-1}$)	Δ	Change (-)
j	Coburn j factor (-)	Ɛ-NTU	Effectiveness-number of transfer units (-)
k	Thermal conductivity ($W\ m^{-1}\ K^{-1}$)	σ	Porosity of heat exchanger (-)
$\dot{m}$	Mass flux ($kg\ m^{-2}\ s^{-1}$)	θ	Cylinder angle (deg)
m	Empirical constant (-)	Subscript	
M	Mass of ammonia absorption (mg)	c	Cross-sectional (-)
n	Empirical constant (-)	d	Diameter of cylinder (-)
Nu	Nusselt number (-)	f	Fluid (-)
OD	Outer diameter (mm)	loc	Local (-)
P	Pressure (Pa)	m	Mean (-)
Pr	Prandtl number (-)	max	Maximum (-)
P_l	Longitudinal tube pitch (mm)	tot	Total (-)
P_t	Transvers tube pitch (mm)	v	Volumetric (-)
P_d	Wave height (mm)	w	Wall (-)
L_d	Slit height (mm)	∞	Free stream flow (-)
ppm	Concentration (parts-per-million)	1,2	Inlet and outlet (-)

REFERENCES

Joardar, A., & Jacobi, A. (2005). Impact of leading edge delta-wing vortex generators on the thermal performance of a flat tube, louvered-fin compact heat exchanger. *International Journal of Heat and Mass Transfer*, 48(8), 1480-1493.

Wang, C. C., Fu, W. L., & Chang, C. T. (1997). Heat transfer and friction characteristics of typical wavy fin-and-tube heat exchangers. *Experimental Thermal and Fluid Science*, 14(2), 174-186.

Wilson, E. E. (1915). A basis for rational design of heat transfer apparatus. *The J Am Soc Mech Engrs*, 37, 546-551.

Che, M., & Elbel, S. (2019). An experimental method to quantify local air-side heat transfer coefficient through mass transfer measurements utilizing color change coatings. *International Journal of Heat and Mass Transfer*, 144, 118624.

Chu, P., He, Y. L., & Tao, W. Q. (2009). Three-dimensional numerical study of flow and heat transfer enhancement using vortex generators in fin-and-tube heat exchangers. *Journal of Heat Transfer*, 131(9).

Chimres, N., Wang, C. C., & Wongwises, S. (2018). Optimal design of the semi-dimple vortex generator in the fin and tube heat exchanger. *International Journal of Heat and Mass Transfer*, 120, 1173-1186.

Wang, C. C., Chen, K. Y., Liaw, J. S., & Tseng, C. Y. (2015). An experimental study of the air-side performance of fin-and-tube heat exchangers having plain, louver, and semi-dimple vortex generator configuration. *International Journal of Heat and Mass Transfer*, 80, 281-287.

Bejan, A. (1995). Convection Heat Transfer, second edition., Wiley, New York.

Krall, K. M., & Eckert, E. R. G. (1973). Local heat transfer around a cylinder at low Reynolds number. *Journal of Heat Transfer*, 95(2), 273-275

Leonard Goland. (1950). A theoretical investigation of heat transfer in the laminar flow regions of airfoils. *Journal of the Aeronautical Sciences*, 17(7), 436-440.

Wang, C. C., Webb, R. L., Chi, K.Y. (2000) Data reduction for air-side performance of fin-and-tube heat exchangers, *Experimental Thermal and Fluid Science*, 21(4) 218-226.

Kays, W.M., London, A.L. (1984). Compact heat exchangers, Krieger Pub., Malabar, FL.

Wang, C. C. (1999). Investigation of wavy fin-and-tube heat exchangers: a contribution to databank. *Experimental Heat Transfer*, 12(1), 73-89.

Jabardo, J. S., Zoghbi Filho, J. B., & Salamanca, A. (2006). Experimental study of the air side performance of louver and wave fin-and-tube coils. *Experimental Thermal and Fluid Science*, 30(7), 621-631.

Okbaz, A., Pınarbaşı, A., & Olcay, A. B. (2020). Experimental investigation of effect of different tube row-numbers, fin pitches and operating conditions on thermal and hydraulic performances of louvered and wavy finned heat exchangers. *International Journal of Thermal Sciences*, 151, 106256.

ACKNOWLEDGEMENTS

The authors would like to thank the member companies of the Air Conditioning and Refrigeration Center at the University of Illinois at Urbana-Champaign for their financial and technical support. The authors would like to thank Creative Thermal Solutions, Inc. (CTS) for providing technical support and equipment. The coating solutions are developed by Serionix, Inc., located in Champaign, IL.